

AN EXTENDED LAGRANGE FEM FOR THE MAXWELL EIGENVALUE PROBLEM

JIAYU HAN

ABSTRACT. We construct an extended Lagrange FE space to solve the Maxwell equation and its eigenvalue problem in \mathbb{R}^d ($d = 2, 3$), which is the sum of the vectorial p -order Lagrange FE space ($p \geq 1$) and the gradient of the $p + 1$ -order Lagrange FE space. The two lowest-order methods in 3D adopt slightly less degrees of freedom than the second family of the same order edge element methods in 3D. We construct a Clément interpolant operator to prove the discrete compactness of the FE space and the convergence of the new methods for both Maxwell equation and its eigenvalue problem. For the extended linear Lagrange element method, an average-type curl recovery approach is designed to obtain numerical solution of super-convergence. In the numerical part, we verify the optimal convergence order for the two lowest-order methods, discuss the upper bound property of numerical eigenvalues and investigate the lower bound property by the average-type curl recovery approach.

Keywords: Maxwell eigenvalue problem, Lagrange finite element, recovery method, eigenvalue upper/lower bound.

1. INTRODUCTION

It is well known that the Nédélec edge elements [1] can approximate the Maxwell eigenvalue problem well in the canonical discrete form. We refer the reader to [2, Section 20] for an extensive survey. However, the direct use of Lagrange finite elements for Maxwell eigenvalue problem will produce erroneous solutions on general meshes (see for example [2, 3]). Two basic approaches to obtain stable discrete schemes include introducing the penalization or regularization terms [4–7] and adopting special meshes [8–12]. The works by Hu et al. [13, 14] developed finite element methods using partially discontinuous Lagrange bases on different meshes. Wong and Cendes [8] adopted Lagrange element methods to obtain the approximation of Maxwell eigenvalues on Powell-Sabin [9] meshes in \mathbb{R}^2 or Worsey-Farin meshes [10] in \mathbb{R}^3 . Recently Boffi et al. [11, 12] theoretically justified this numerical fact.

To enforce the div-free constraint, the Maxwell eigenvalue problem can be discretized as mixed forms (c.f. [11, 12, 15–19]). However, the canonical mixed form using the Lagrange finite element space is not stable. Our research aims at proposing an extended Lagrange element method to fill this gap. To do this, we extend the vectorial p -order Lagrange element space $\mathbf{L}_{h,0}$ with the gradient of its $p + 1$ -order space U_h ($p \geq 1$). The extended FE methods in low order cases have slightly less degrees of freedom than the second family of edge element methods. In order to accomplish the error analysis, we prove the discrete compactness of the extended spaces $\mathbf{L}_{h,0} + \nabla U_h$ and the pointwise convergence of the discrete solution operator. Then the optimal convergence order of the discrete eigen-pairs is obtained by the Babuška-Osborn theory [20].

In addition, we propose an average-type curl recovery scheme for the extended linear Lagrange element method. We can verify that when the Maxwell eigenfunction is smooth,

This work is partially supported by the National Natural Science Foundation of China (under Grants 12361084 and 12001130).

the numerical eigenvalue approximates the exact one from upper (see section 5.2). Then this scheme can be used to obtain the supercloseness lower bound of the exact eigenvalues. For the other work of the numerical lower bound of Maxwell eigenvalues we refer the reader to [21]; we also refer the reader to [22–25] for other related early works.

To the best of our knowledge, the proposed methods seem to be the first effective work using the canonical discrete form and Lagrange element spaces on general simplicial meshes in both 2D and 3D. It is worth noting that the finite element programs using Lagrange element spaces have been well exploited on existing softwares.

We organize this paper as follows. In Section 2, we introduce the extended Lagrange element spaces, the canonical discrete formulation and its equivalent mixed formulation. In Section 3, we prove the discrete compactness of the extended Lagrange element space and the pointwisely convergence of the discrete solution operators. Then we derive the optimal convergence order of the discrete eigen-pairs. In Section 4, we design a average type curl recovery scheme for the extended linear Lagrange elements. In the last section, we verify numerically the theoretical results using the two lowest order methods in both 2D and 3D.

2. EXTENDED LAGRANGE ELEMENT DISCRETIZATION

We consider the shape regular and affine meshes $\mathcal{T}_h = \{K\}$ that partition the simply-connected Lipschitz domain $\Omega \subset \mathbb{R}^d$ ($d = 2, 3$) into triangles or tetrahedra in \mathbb{R}^d . The extended Lagrange finite element spaces in this paper is given as

$$(2.1) \quad \mathbf{V}_h = \mathbf{L}_{h,0} + \nabla U_h$$

where

$$\begin{aligned} \mathbf{L}_h &= \{\mathbf{q}_h \in (H^1(\Omega))^d \mid \mathbf{q}_h|_K \in (P_p(K))^d, \forall K \in \mathcal{T}_h\}, \\ \mathbf{L}_{h,0} &= \{\mathbf{q}_h \in \mathbf{L}_h \mid \mathbf{q}_h \times \mathbf{n} = 0 \text{ on } \partial\Omega\}, \\ U_h &= \{q_h \in H_0^1(\Omega) \mid q_h|_K \in P_{p+1}(K), \forall K \in \mathcal{T}_h\}, \quad p \geq 1. \end{aligned}$$

The Lagrange FE space $\mathbf{L}_{h,0}$ provides the approximation property of piecewise p -degree polynomials and the gradient space ∇U_h provides the tangential continuity.

Consider the Maxwell eigenvalue problem : Find $(\lambda, \mathbf{u}) \in \mathbb{R} \times \mathbf{H}_0(\text{curl}, \Omega) \setminus \{0\}$ such that

$$(2.2) \quad (\text{curl} \mathbf{u}, \text{curl} \mathbf{v}) = \lambda(\mathbf{u}, \mathbf{v}), \quad \forall \mathbf{v} \in \mathbf{H}_0(\text{curl}, \Omega).$$

We introduce the space

$$\mathbf{H}_0(\text{curl}, \Omega) := \{\mathbf{v} \in \mathbf{L}^2(\Omega) : \text{curl} \mathbf{v} \in \mathbf{L}^2(\Omega) \text{ and } \mathbf{v} \times \mathbf{n} = 0 \text{ on } \partial\Omega\},$$

equipped with the standard norm $\|\cdot\|_{\text{curl}}$. Here \mathbf{n} is a unit outward normal vector on $\partial\Omega$.

The Maxwell eigenvalue problem can be also written as: Find $(\lambda, \mathbf{u}) \in \mathbb{R} \times \mathbf{H}_0(\text{curl}, \Omega) \setminus \{0\}$ and $\rho \in H_0^1(\Omega)$ such that

$$(2.3) \quad \begin{aligned} (\text{curl} \mathbf{u}, \text{curl} \mathbf{v}) + (\nabla \rho, \mathbf{v}) &= \lambda(\mathbf{u}, \mathbf{v}), \quad \forall \mathbf{v} \in \mathbf{H}_0(\text{curl}, \Omega), \\ (\mathbf{u}, \nabla q) &= 0, \quad \forall q \in H_0^1(\Omega). \end{aligned}$$

Accordingly, the extended Lagrange finite element method with respect to the FE space $\mathbf{V}_h \subset \mathbf{H}_0(\text{curl}, \Omega)$ is to find $\mathbf{u}_h \in \mathbf{V}_h \setminus \{0\}$ and nonzero $\lambda_h \in \mathbb{R}$ such that

$$(2.4) \quad (\text{curl} \mathbf{u}_h, \text{curl} \mathbf{v}_h) = \lambda_h(\mathbf{u}_h, \mathbf{v}_h), \quad \forall \mathbf{v}_h \in \mathbf{V}_h$$

An equivalent discrete form of the eigenvalue problem (2.4) is given by: Find $(\lambda_h, \mathbf{u}_h, \rho_h) \in \mathbb{R} \times \mathbf{V}_h \times U_h$ with $\mathbf{u}_h \neq 0$ such that

$$(2.5) \quad \begin{aligned} (\operatorname{curl} \mathbf{u}_h, \operatorname{curl} \mathbf{v}_h) + (\nabla \rho_h, \mathbf{v}_h) &= \lambda_h (\mathbf{u}_h, \mathbf{v}_h), \quad \forall \mathbf{v}_h \in \mathbf{V}_h, \\ (\mathbf{u}_h, \nabla q) &= 0, \quad \forall q \in U_h. \end{aligned}$$

It is easy to see that $\rho_h = 0$.

3. ERROR ANALYSIS

First we shall construct a Clément interpolant operator [26] adapted to the boundary condition $\mathbf{v} \times \mathbf{n} = 0$ on $\partial\Omega$. Let Δ_i denote the union set of elements sharing the i th node and $\widehat{\Delta}_i$ denote its reference element satisfying the linear transformation $\mathbf{x} = F_{\Delta_i}(\widehat{\mathbf{x}}) = B_{\Delta_i} \widehat{\mathbf{x}} + b_{\Delta_i}$. Define the operator $\widehat{\mathbf{R}}_i : L^1(\widehat{\Delta}_i) \rightarrow \mathbf{P}_k(\widehat{\Delta}_i)$ satisfying

$$(3.1) \quad \int_{\widehat{\Delta}_i} (\widehat{\mathbf{R}}_i \widehat{\mathbf{v}} - \widehat{\mathbf{v}}) \cdot \widehat{\mathbf{p}} = 0, \quad \forall \widehat{\mathbf{p}} \in \mathbf{P}_k(\widehat{\Delta}_i).$$

For $\mathbf{v} \in \mathbf{L}^1(\Omega)$ we define $\Pi_h : \mathbf{L}^1(\Omega) \rightarrow \mathbf{L}_h$ as follows:

$$(3.2) \quad \Pi_h \mathbf{v} = \sum_{i=1}^{N_h} \mathbf{R}_i \mathbf{v}(\mathbf{x}) \theta_i$$

where $\mathbf{R}_i \mathbf{v}(\mathbf{x}) := \widehat{\mathbf{R}}_i \widehat{\mathbf{v}}(\widehat{\mathbf{x}})$, $N_h = \dim \mathbf{L}_h$ and θ_i is the Lagrange basis corresponding to the i th node in the mesh \mathcal{T}_h .

Hereafter we denote the standard Sobolev space $\mathbf{W}^{s,q}(D)$ on a bounded Lipschitz domain D equipped with the norm $\|\cdot\|_{s,q,D}$. Let $\mathbf{H}^s(D) := \mathbf{W}^{s,2}(D)$. In this paper, we use the symbol $x \lesssim y$ ($x \gtrsim y$) to mean $x \leq Cy$ ($x \geq Cy$) for a constant C that is independent of the mesh size and may be different at different occurrences.

Let $\mathbf{v} \in \mathbf{H}^s(\Delta_i)$ with $0 \leq m \leq s \leq p+1$. Pick up any $K \subset \Delta_i$. By the scaling argument and norm equivalence

$$(3.3) \quad |\mathbf{R}_i \mathbf{v} - \mathbf{v}|_{m,K} \lesssim h_{\Delta_i}^{\frac{d}{2}-m} \inf_{\widehat{\mathbf{q}} \in \mathbf{P}_k(\widehat{K})} |(\widehat{\mathbf{R}}_i - I)(\widehat{\mathbf{v}} + \widehat{\mathbf{q}})|_{m,\widehat{\Delta}_i} \lesssim h_{\Delta_i}^{\frac{d}{2}-m} |\widehat{\mathbf{v}}|_{s,\widehat{\Delta}_i} \lesssim h_{\Delta_i}^{s-m} |\mathbf{v}|_{s,\Delta_i}.$$

Assume that the FE nodes $a_{i_1}, \dots, a_{i_\alpha}$ belong to the element K . By inverse estimate we derive

$$(3.4) \quad \begin{aligned} |\mathbf{R}_{i_1} \mathbf{v} - \Pi_h \mathbf{v}|_{m,K} &\leq \sum_{j=2}^{\alpha} \|\theta_{i_j} (\mathbf{R}_{i_1} \mathbf{v}(a_{i_j}) - \mathbf{R}_{i_j} \mathbf{v}(a_{i_j}))\|_{m,K} \\ &\lesssim h_{\Delta_i}^{\frac{d}{2}-m} \sum_{j=2}^{\alpha} \|\mathbf{R}_{i_1} \mathbf{v} - \mathbf{R}_{i_j} \mathbf{v}\|_{\infty,K} \\ &\lesssim h_{\Delta_i}^{-m} \sum_{j=2}^{\alpha} \|\mathbf{R}_{i_1} \mathbf{v} - \mathbf{R}_{i_j} \mathbf{v}\|_{0,K} \\ &\lesssim h_{\Delta_i}^{s-m} |\mathbf{v}|_{s,\Delta_i} \text{ by (3.3)}. \end{aligned}$$

The combination of the above two estimates gives

$$(3.5) \quad |\Pi_h \mathbf{v} - \mathbf{v}|_{m,K} \leq |\mathbf{R}_{i_1} \mathbf{v} - \mathbf{v}|_{m,K} + |\mathbf{R}_{i_1} \mathbf{v} - \Pi_h \mathbf{v}|_{m,K} \lesssim h_{\Delta_i}^{s-m} |\mathbf{v}|_{s,\Delta_i}.$$

We divide the Lagrange bases into two classes: the interior nodal bases $\{\theta_i\}_{i=1}^{N_{h0}}$ and the boundary nodal bases $\{\theta_i\}_{i=1+N_{h0}}^{N_h}$. For $\mathbf{v} \in \mathbf{L}^1(\Omega)$ we define $\Pi_{h,0} : \mathbf{L}^1(\Omega) \rightarrow \mathbf{L}_{h,0}$ as follows:

$$(3.6) \quad \Pi_{h,0}\mathbf{v} = \sum_{i=1}^{N_{h0}} \mathbf{R}_i \mathbf{v}(a_i) \theta_i + \sum_{i=1+N_{h0}}^{N_h} J\mathbf{v}(a_i) \theta_i$$

where

$$(3.7a) \quad J\mathbf{v}(a_i) = (\mathbf{R}_i \mathbf{v}(a_i) \cdot \mathbf{n}|_{f_1}(a_i)) \mathbf{n}|_{f_1}(a_i), \quad \mathbf{n}|_{f_1}(a_i) = \mathbf{n}|_{f_2}(a_i) \text{ and } a_i \in f_1 \cap f_2 \subset \partial\Omega,$$

$$(3.7b) \quad J\mathbf{v}(a_i) = 0, \quad \mathbf{n}|_{f_1}(a_i) \neq \mathbf{n}|_{f_2}(a_i) \text{ and } a_i \in f_1 \cap f_2 \subset \partial\Omega,$$

$$(3.7c) \quad J\mathbf{v}(a_i) = (\mathbf{R}_i \mathbf{v}(a_i) \cdot \mathbf{n}|_f(a_i)) \mathbf{n}|_f(a_i), \quad a_i \in f \subset \partial\Omega \text{ and } a_i \notin \text{any other face,}$$

f is an face of \mathcal{T}_h in \mathbb{R}^3 (or an edge in \mathbb{R}^2), and f_1 and f_2 are two different faces in \mathbb{R}^3 (or edges in \mathbb{R}^2).

Lemma 3.1. For $\mathbf{v} \in \mathbf{H}^s(\Omega) \cap \mathbf{H}_0(\text{curl}, \Omega)$ with $p+1 \geq s > 1/2$ there holds

$$(3.8) \quad |\Pi_{h,0}\mathbf{v} - \mathbf{v}|_{m,K} \lesssim h_{\Delta_i}^{s-m} |\mathbf{v}|_{s,\Delta_i} \text{ for } 0 \leq m \leq s.$$

Proof. Let the element K satisfy $\overline{K} \cap \partial\Omega \neq \emptyset$ and there are β nodes i_1, \dots, i_β of K on $\partial\Omega$. For any integer $j \in [1, \beta]$ and $a_{i_j} \in \partial\Omega \cap \partial K$ we have

$$(\Pi_h \mathbf{v} - \Pi_{h,0}\mathbf{v})(a_{i_j}) = \begin{cases} \sum_{j=1}^{\beta} \sum_{k=1}^{d-1} \mathbf{R}_{i_j} \mathbf{v}(a_{i_j}) \cdot \boldsymbol{\tau}_k(a_{i_j}) \boldsymbol{\tau}_k(a_{i_j}), & \text{if } a_{i_j} \text{ satisfies (3.7a) and (3.7c)} \\ \mathbf{R}_{i_j} \mathbf{v}(a_{i_j}), & \text{if } a_{i_j} \text{ satisfies (3.7b)} \end{cases}$$

where $\boldsymbol{\tau}_k(a_{i_j})$ is the k th tangent direction at the node a_{i_j} . Pick up $\sigma > 0$ such that $\sigma + 1/2 \leq s$. Note that $\mathbf{v} \times \mathbf{n}|_{\partial\Omega} = 0$ then

$$(3.9) \quad \begin{aligned} |\Pi_{h,0}\mathbf{v} - \Pi_h \mathbf{v}|_{m,K} &\lesssim \sum_{j=1}^{\beta} \sum_{k=1}^{d-1} \|\Pi_{h,0}\mathbf{v}(a_{i_j}) - \Pi_h \mathbf{v}(a_{i_j})\| \|\theta_{i_j}\|_{m,K} \\ &\lesssim h_{\Delta_i}^{\frac{1}{2}-m} \sum_{j=1}^{\beta} \|\mathbf{R}_{i_j} \mathbf{v} - \mathbf{v}\|_{0,\partial K \cap \partial\Omega} \\ &\lesssim h_{\Delta_i}^{\frac{d}{2}-m} \sum_{j=1}^{\beta} \inf_{\mathbf{q} \in P_k(\widehat{K})} \|(\widehat{\mathbf{R}}_{i_j} - I)(\widehat{\mathbf{v}} + \mathbf{q})\|_{1/2+\sigma,\widehat{K}} \\ &\lesssim h_{\Delta_i}^{s-m} |\mathbf{v}|_{s,\Delta_i}. \end{aligned}$$

This together with (3.5) yields

$$(3.10) \quad |\Pi_{h,0}\mathbf{v} - \mathbf{v}|_{m,K} \leq |\Pi_h \mathbf{v} - \mathbf{v}|_{m,K} + |\Pi_{h,0}\mathbf{v} - \Pi_h \mathbf{v}|_{m,K} \lesssim h_{\Delta_i}^{s-m} |\mathbf{v}|_{s,\Delta_i}.$$

□

The Hodge operator is a useful tool in our error analysis. It is defined as $H\mathbf{g} \in \mathbf{H}_0(\text{curl}, \Omega)$ and $\varrho \in H_0^1(\Omega)$ for $\mathbf{g} \in \mathbf{H}_0(\text{curl}, \Omega)$ such that

$$(3.11) \quad \begin{aligned} (\text{curl} H\mathbf{g}, \text{curl} \mathbf{v}) + (\nabla \varrho, \mathbf{v}) &= (\text{curl} \mathbf{g}, \text{curl} \mathbf{v}), \quad \forall \mathbf{v} \in \mathbf{H}_0(\text{curl}, \Omega), \\ (\nabla q, H\mathbf{g}) &= 0, \quad \forall q \in H_0^1(\Omega). \end{aligned}$$

We introduce the following curl-conforming element spaces [1]:

$$(3.12) \quad \tilde{\mathbf{V}}_h := \{\mathbf{v}_h \in \mathbf{H}_0(\text{curl}, \Omega) | \mathbf{v}_h|_K \in (P_p(K))^d, \forall K \in \mathcal{T}_h\} \supset \mathbf{V}_h,$$

$$(3.13) \quad \mathbf{X}_h := \{\mathbf{v}_h \in \mathbf{V}_h | (\mathbf{v}_h, \nabla q) = 0, \forall q \in U_h\},$$

$$(3.14) \quad \mathbf{X} := \{\mathbf{v} \in \mathbf{H}_0(\text{curl}, \Omega) | (\mathbf{v}, \nabla q) = 0, \forall q \in H_0^1(\Omega)\},$$

Let λ^{Dir} be the minimum singularity exponents for the Dirichlet Laplace operators, and satisfy

$$(3.15) \quad \{\psi \in H_0^1(\Omega) : \Delta\psi \in L^2(\Omega), \} \subset \bigcap_{s < \lambda^{Dir}} H^{1+s}(\Omega).$$

We give the interpolation error estimates corresponding to the above finite element spaces.

Lemma 3.2 (Theorem 5.41 in [15]). *Let r_h be the edge element interpolation associated with $\tilde{\mathbf{V}}_h$ and $\mathbf{v}, \text{curl}\mathbf{v} \in \mathbf{H}^s(\Omega)$ ($p \geq s > 1/2$) then*

$$(3.16) \quad \|r_h\mathbf{v} - \mathbf{v}\|_{\text{curl}} \lesssim h^s (\|\mathbf{v}\|_{s,\Omega} + \|\text{curl}\mathbf{v}\|_{s,\Omega}).$$

Let $\mathbf{v} \in \mathbf{X} \subset \mathbf{H}^{r_D}(\Omega)$ for $r_D := \lambda^{Dir} - \varepsilon$ with sufficiently small $\varepsilon > 0$ and $\text{curl}\mathbf{v} \in \text{curl}\tilde{\mathbf{V}}_h$ then

$$(3.17) \quad \|r_h\mathbf{v} - \mathbf{v}\| \lesssim h^{r_D} (\|\mathbf{v}\|_{r_D,\Omega} + \|\text{curl}\mathbf{v}\|).$$

Lemma 3.3. *Let $\mathbf{v}_h \in \mathbf{X}_h$ then $H\mathbf{v}_h \in \mathbf{X}$ such that $\text{curl}\mathbf{v}_h = \text{curl}H\mathbf{v}_h$ and*

$$(3.18) \quad \|H\mathbf{v}_h\|_{r_D,\Omega} \lesssim \|\text{curl}\mathbf{v}_h\|,$$

$$(3.19) \quad \|H\mathbf{v}_h - \mathbf{v}_h\| \leq \|r_h H\mathbf{v}_h - H\mathbf{v}_h\|.$$

Proof. The proof follows Lemma 7.6 in [15] or Lemma 4.5 in [17]. The regularity estimate (3.18) is due to $\mathbf{X} \subset \mathbf{H}^{r_D}(\Omega)$ (c.f. Remark 3.8 in [27]). According to the definition of H , we have $\text{curl}H\mathbf{v}_h = \text{curl}\mathbf{v}_h$. By the commuting property of r_h we have $\text{curl}(r_h H\mathbf{v}_h) = \text{curl}\mathbf{v}_h$. This implies $r_h H\mathbf{v}_h - \mathbf{v}_h \in \nabla U_h$ (see Section 7.2.1 in [15]). According to $(H\mathbf{v}_h - \mathbf{v}_h, \mathbf{q}) = 0, \forall \mathbf{q} \in \nabla U_h$, we have $(H\mathbf{v}_h - \mathbf{v}_h, r_h H\mathbf{v}_h - \mathbf{v}_h) = 0$. Hence using Lemma 3.2 we deduce

$$\begin{aligned} (H\mathbf{v}_h - \mathbf{v}_h, H\mathbf{v}_h - \mathbf{v}_h) &= (H\mathbf{v}_h - r_h H\mathbf{v}_h, H\mathbf{v}_h - \mathbf{v}_h) \\ &\lesssim \|H\mathbf{v}_h - \mathbf{v}_h\| (h^{r_D} \|H\mathbf{v}_h\|_{r_0,\Omega} + h \|\text{curl}\mathbf{v}_h\|). \end{aligned}$$

Then the estimate (3.19) is obtained by the above estimate and (3.18). \square

To analyze the convergence of the discretization (2.5), we consider the source problem with div-free constraint: Find $T\mathbf{f} \in \mathbf{H}_0(\text{curl}, \Omega)$ and $S\mathbf{f} \in H_0^1(\Omega)$ such that

$$(3.20) \quad \begin{aligned} (\text{curl}T\mathbf{f}, \text{curl}\mathbf{v}) + (\nabla S\mathbf{f}, \mathbf{v}) &= (\mathbf{f}, \mathbf{v}), \quad \forall \mathbf{v} \in \mathbf{H}_0(\text{curl}, \Omega), \\ (\nabla q, T\mathbf{f}) &= 0, \quad \forall q \in H_0^1(\Omega). \end{aligned}$$

Its extended Lagrange FE discretization is to seek $T_h\mathbf{f} \in \mathbf{V}_h$ and $S_h\mathbf{f} \in U_h$:

$$(3.21) \quad \begin{aligned} (\text{curl}T_h\mathbf{f}, \text{curl}\mathbf{v}_h) + (\nabla S_h\mathbf{f}, \mathbf{v}_h) &= (\mathbf{f}, \mathbf{v}_h), \quad \forall \mathbf{v}_h \in \mathbf{V}_h, \\ (\nabla q, T_h\mathbf{f}) &= 0, \quad \forall q \in U_h. \end{aligned}$$

It is easy to verify that $S\mathbf{f} = S_h\mathbf{f} = 0$ for any $\mathbf{f} \in \mathbf{X}$. Let $\mathbf{f} = 0$ then $T_h\mathbf{f} \in \nabla U_h$ and so $T_h\mathbf{f} = 0$. Therefore the problem (3.21) is uniquely solvable.

Let $\lambda^{Neu} \in (1/2, 1]$ be the minimum singularity exponents for the Neumann Laplace operators, and satisfy

$$(3.22) \quad \left\{ \psi \in H^1(\Omega) : \Delta\psi \in L^2(\Omega), \frac{\partial\psi}{\partial n} = 0 \text{ on } \partial\Omega, \int_{\Omega} \psi dx = 0 \right\} \subset \bigcap_{s < \lambda^{Neu}} H^{1+s}(\Omega).$$

Lemma 3.4 (Corollary 6.4 in [28]). *There holds the following decomposition for $T\mathbf{f}$ in the equation (3.20):*

$$(3.23) \quad T\mathbf{f} = \mathbf{w}_0 + \nabla\phi \text{ with } \mathbf{w}_0 \in \mathbf{H}^{1+\lambda^{Neu}-\varepsilon_1}(\Omega) \text{ and } \phi \in H_0^1(\Omega) \cap H^{1+\lambda^{Dir}-\varepsilon_2}(\Omega)$$

where $\varepsilon_1, \varepsilon_2 > 0$ arbitrarily approach to 0.

Since $\text{curl}^2 T\mathbf{f} = -\nabla S\mathbf{f} + \mathbf{f}$, by the above lemma we have $T\mathbf{f}, \text{curl} T\mathbf{f} \in \mathbf{H}^r(\Omega)$ for some $r \geq r_0$ with r_0 given by the following theorem.

Theorem 3.5. *Let $\mathbf{f} \in \mathbf{L}^2(\Omega)$, $T\mathbf{f} \in \mathbf{H}^r(\Omega)$ and $\mathbf{w}_0 \in \mathbf{H}^{r+1}(\Omega)$ for $p \geq r \geq r_0 := \min(\lambda^{Dir}, \lambda^{Neu}) - \varepsilon$ with sufficiently small $\varepsilon > 0$ then*

$$(3.24) \quad \|(T - T_h)\mathbf{f}\|_{\text{curl}} \lesssim h^r + \inf_{\mathbf{v}_h \in U_h} |S\mathbf{f} - \mathbf{v}_h|_{1,\Omega};$$

further assume $T\mathbf{f} \in \mathbf{H}^s(\Omega)$ for $r \leq s \leq r_0 + r \leq r_0 + p$ and $\text{div} \mathbf{f} = 0$ then

$$(3.25) \quad \|T\mathbf{f} - T_h\mathbf{f}\| \lesssim h^s.$$

Proof. The combination of (3.20) and (3.21) leads to

$$(\text{curl}(T - T_h)\mathbf{f}, \text{curl} \mathbf{v}_h) + (\nabla(S - S_h)\mathbf{f}, \mathbf{v}_h) = 0, \quad \forall \mathbf{v}_h \in \mathbf{V}_h.$$

It follows that

$$\begin{aligned} (\text{curl}(\mathbf{v}_h - T_h\mathbf{f}), \text{curl}(\mathbf{v}_h - T_h\mathbf{f})) &= (\text{curl}(\mathbf{v}_h - T\mathbf{f}), \text{curl}(\mathbf{v}_h - T_h\mathbf{f})) \\ &\quad - (\nabla(S - S_h)\mathbf{f}, \mathbf{v}_h - T_h\mathbf{f}), \quad \forall \mathbf{v}_h \in \mathbf{X}_h. \end{aligned}$$

Hence we have from the Poincaré inequality in \mathbf{X}_h and $\mathbf{V}_h = \mathbf{X}_h \oplus \nabla U_h$

$$\|\text{curl}(\mathbf{v}_h - T_h\mathbf{f})\| \lesssim \|\text{curl}(T\mathbf{f} - \mathbf{v}_h)\| + |(S - S_h)\mathbf{f}|_{1,\Omega}, \quad \forall \mathbf{v}_h \in \mathbf{V}_h.$$

Taking \mathbf{v}_h as $\mathbf{\Pi}_{h,0}\mathbf{w}_0$, this together with the triangular inequality infers that

$$\|\text{curl}(T\mathbf{f} - T_h\mathbf{f})\| \lesssim \|\text{curl}(\mathbf{w}_0 - \mathbf{\Pi}_{h,0}\mathbf{w}_0)\| + |(S - S_h)\mathbf{f}|_{1,\Omega} \lesssim h^r + |(S - S_h)\mathbf{f}|_{1,\Omega}.$$

Let P_h be the orthogonal projection onto $\tilde{\mathbf{V}}_h$ such that for any $\mathbf{v} \in \mathbf{H}_0(\text{curl}, \Omega)$

$$(3.26) \quad (\mathbf{v} - P_h\mathbf{v}, \mathbf{q}) + (\text{curl}(\mathbf{v} - P_h\mathbf{v}), \text{curl} \mathbf{q}) = 0, \quad \forall \mathbf{q} \in \tilde{\mathbf{V}}_h.$$

By the triangular inequality and the discrete Poincaré inequality we get

$$\begin{aligned} \|T\mathbf{f} - T_h\mathbf{f}\| &\lesssim \|T\mathbf{f} - P_h T\mathbf{f}\| + \|\text{curl}(P_h T\mathbf{f} - T_h\mathbf{f})\| \\ &\lesssim \|T\mathbf{f} - P_h T\mathbf{f}\|_{\text{curl}} + \|\text{curl}(T\mathbf{f} - T_h\mathbf{f})\|. \end{aligned}$$

This together with the above estimate and (3.16) leads to the conclusion (3.24). We have the following Helmholtz decomposition $r_h T\mathbf{f} - T_h\mathbf{f} = \mathbf{w}_0^c + \nabla q_h$ with $\mathbf{w}_0^c \in \tilde{\mathbf{V}}_h$, $(\mathbf{w}_0^c, \nabla q) = 0, \forall q \in U_h$ and $q_h \in U_h$. For $\mathbf{f} \in \mathbf{L}^2(\Omega)$ with $\text{div} \mathbf{f} = 0$, we start as follows

$$(3.27) \quad \begin{aligned} \|T\mathbf{f} - T_h\mathbf{f}\|^2 &= (T\mathbf{f} - T_h\mathbf{f}, T\mathbf{f} - r_h T\mathbf{f} + r_h T\mathbf{f} - T_h\mathbf{f}) \\ &\lesssim \|T\mathbf{f} - r_h T\mathbf{f}\| \|T\mathbf{f} - T_h\mathbf{f}\| + |(T\mathbf{f} - T_h\mathbf{f}, \mathbf{w}_0^c)|. \end{aligned}$$

Note that $S_h H \mathbf{w}_0^c = S H \mathbf{w}_0^c = 0$. Using Lemmas 3.2-3.4, the second term at the right-hand side is estimated as follows:

$$(3.28) \quad \begin{aligned} |(T\mathbf{f} - T_h\mathbf{f}, \mathbf{w}_0^c)| &\lesssim |(T\mathbf{f} - T_h\mathbf{f}, \mathbf{w}_0^c - H\mathbf{w}_0^c)| + |(T\mathbf{f} - T_h\mathbf{f}, H\mathbf{w}_0^c)| \\ &\lesssim h^{r_0} \|\operatorname{curl} \mathbf{w}_0^c\| \|T\mathbf{f} - T_h\mathbf{f}\| + |(T\mathbf{f} - T_h\mathbf{f}, H\mathbf{w}_0^c)| \text{ by (3.19), (3.17) and (3.18)} \end{aligned}$$

where

$$(3.29) \quad \begin{aligned} |(T\mathbf{f} - T_h\mathbf{f}, H\mathbf{w}_0^c)| &= (\operatorname{curl}(T\mathbf{f} - T_h\mathbf{f}), \operatorname{curl}(TH\mathbf{w}_0^c - \mathbf{\Pi}_{h,0} TH\mathbf{w}_0^c)) \\ &\lesssim h^{r_0} \|H\mathbf{w}_0^c\| \|\operatorname{curl}(T\mathbf{f} - T_h\mathbf{f})\| \text{ by Lem. 3.1 and (3.23)} \\ &\lesssim h^{r_0} (h^{r_D} \|\operatorname{curl} \mathbf{w}_0^c\| + \|\mathbf{w}_0^c\|) \|\operatorname{curl}(T\mathbf{f} - T_h\mathbf{f})\| \text{ by (3.19)} \\ &\lesssim (h^{r_0} \|\operatorname{curl}(r_h T\mathbf{f} - T_h\mathbf{f})\| + \|r_h T\mathbf{f} - T_h\mathbf{f}\|) \|\operatorname{curl}(T\mathbf{f} - T_h\mathbf{f})\| h^{r_0}. \end{aligned}$$

The substitution of (3.29) and (3.28) into (3.27) gives

$$(3.30) \quad \begin{aligned} \|T\mathbf{f} - T_h\mathbf{f}\| &\lesssim h^{r_0} \|\operatorname{curl}(T\mathbf{f} - T_h\mathbf{f})\| + h^{r_0} \|\operatorname{curl}(r_h T\mathbf{f} - T\mathbf{f} + T\mathbf{f} - T_h\mathbf{f})\| + \|r_h T\mathbf{f} - T\mathbf{f}\| \\ &\lesssim h^{r_0+r} + h^s \text{ by (3.24) and Lemma 3.1,} \end{aligned}$$

where we have used $\|r_h T\mathbf{f} - T\mathbf{f}\| \lesssim h^s \|T\mathbf{f}\|_{s,\Omega}$ (see Theorem 8.15 in [15]). This completes the proof. \square

Let \mathcal{H} be a sequence of the mesh sizes converging to 0.

Lemma 3.6. (*Discrete compactness property*) Any sequence $\{\mathbf{v}_h\}_{h \in \mathcal{H}}$ with $\mathbf{v}_h \in \mathbf{X}_h$ that is uniformly bounded w.r.t $\|\cdot\|_{\operatorname{curl}}$ contains a subsequence that converges strongly in $\mathbf{L}^2(\Omega)$.

Proof. Let $\{\mathbf{v}_h\}_{h \in \mathcal{H}}$ with $\|\mathbf{v}_h\|_{\operatorname{curl}} \leq M$ for a positive constant M . It is trivial to assume that the sequece $h_i \in \mathcal{H}$ satisfies $h_i \rightarrow 0$ as $i \rightarrow \infty$. By (3.19), (3.17) and (3.18), $\|H\mathbf{v}_{h_i} - \mathbf{v}_{h_i}\| \lesssim h^{r_0} \|\operatorname{curl} \mathbf{v}_{h_i}\| \rightarrow 0$ as $i \rightarrow \infty$. Note that

$$\|\operatorname{curl} H\mathbf{v}_{h_i}\| = \|\operatorname{curl} \mathbf{v}_{h_i}\| \leq M.$$

This means that $\{H\mathbf{v}_{h_i}\}$ is bounded in $\mathbf{H}(\operatorname{curl}, \Omega)$. Since \mathbf{X} is compactly imbedded into $\mathbf{L}^2(\Omega)$, there is a subsequence of $\{H\mathbf{v}_{h_i}\}$ converging to some \mathbf{v}_0 in $\mathbf{L}^2(\Omega)$. Hence a subsequence of $\{\mathbf{v}_{h_i}\}$ will converge to \mathbf{v}_0 in $\mathbf{L}^2(\Omega)$ as well. \square

The following uniform convergence can be derived from the discrete compactness property of \mathbf{X}_h .

Theorem 3.7. *There holds the uniform convergence*

$$\|T_h - T\|_{\mathbf{L}^2(\Omega) \rightarrow \mathbf{L}^2(\Omega)} \rightarrow 0, \quad h \rightarrow 0.$$

Proof. Since $\cup_{h \in \mathcal{H}} U_h$ is dense in $H_0^1(\Omega)$, we deduce from Theorem 3.5 that T_h converges to T pointwisely in $\mathbf{L}^2(\Omega)$. Thanks to the discrete compactness of \mathbf{X}_h , $\cup_{h \in \mathcal{H}} T_h B a$ is a relatively compact set in $\mathbf{L}^2(\Omega)$ where $B a$ is the unit ball in $\mathbf{L}^2(\Omega)$. In fact, Let us choose any sequence $\{\mathbf{v}_h\}_{h \in \mathcal{H}} \subset B a$. Note that T is compact from \mathbf{X} to $\mathbf{L}^2(\Omega)$ then $\{T\mathbf{v}_h\}_{h \in \mathcal{H}}$ is a relatively compact set in $\mathbf{L}^2(\Omega)$. Hence it holds the collectively compact convergence $T_h \rightarrow T$ in $\mathbf{L}^2(\Omega)$ as $h \rightarrow 0$. Noting $T, T_h : \mathbf{L}^2(\Omega) \rightarrow \mathbf{L}^2(\Omega)$ are self-adjoint, due to Proposition 3.7 or Table 3.1 in [29] the assertion is valid. \square

We are in a position to prove the error estimate for the numerical eigenvalues.

Theorem 3.8. *Let λ_h be an eigenvalue of (2.4) converging to the eigenvalue λ of (2.3). Under the condition of theorem 3.5, let $M(\lambda) \subset \{\mathbf{u} \in \mathbf{H}^r(\Omega) : \mathbf{u} \in \mathbf{H}^{r+1}(\Omega) + \nabla H_0^1(\Omega)\}$ for some $r \in [r_0, p]$ then*

$$(3.31) \quad |\lambda - \lambda_h| \lesssim h^{2r},$$

where $M(\lambda)$ denotes the space spanned by all eigenfunctions corresponding to the eigenvalue λ .

Proof. Let $\lambda = \lambda_k$ be the k th Maxwell eigenvalue and $\dim M(\lambda) = q$. From Theorem 7.3 in [20] we get

$$(3.32) \quad |\lambda - \lambda_h| \lesssim \sum_{i,j=k}^{k+q-1} |((T - T_h)\phi_i, \phi_j)| + \|(T - T_h)|_{M(\lambda)}\|_{\mathbf{L}^2(\Omega) \rightarrow \mathbf{L}^2(\Omega)}^2,$$

where $\phi_k, \dots, \phi_{k+q-1}$ are a set of basis functions for $M(\lambda)$. Note that $S\mathbf{f} = S_h\mathbf{f} = 0$ for any $\mathbf{f} \in \mathbf{X}$ in (3.20) and (3.21). Hence the following Galerkin orthogonality holds:

$$((T - T_h)\phi_i, \phi_j) = (\text{curl}(T - T_h)\phi_i, \text{curl}T\phi_j) = (\text{curl}(T - T_h)\phi_i, \text{curl}(T - T_h)\phi_j).$$

Substituting this into (3.32), we deduce (3.31) from (3.24). \square

4. SUPER-CONVERGENCE OF AVERAGE-TYPE CURL RECOVERY SCHEME IN EXTENDED LINEAR LAGRANGE ELEMENT

We define \mathcal{N}_h as the nodal set of a quasi-uniform triangulation \mathcal{T}_h . Given $z \in \mathcal{N}_h$, we consider an element patch ω_z around z where we choose as the origin of a local coordinates. Under this coordinate system, we let z be the barycenter of a simplex $K_j \subset \omega_z, j = 1, 2, \dots, m_z$, where m_z is the number of elements containing the vertex z .

Next we shall propose an average type curl recovery scheme, which is a similar version as in [30]. Let us define the simple averaging operator $C_h : \{\mathbf{v} \in \mathbf{H}_0(\text{curl}, \Omega) : \mathbf{curl}(\mathbf{v}|_{\overline{K}}) \in \mathbf{C}^0(\overline{K}), \forall K \in \mathcal{T}_h\} \mapsto \mathbf{L}_h$ as follows:

$$C_h \mathbf{u}_h(z) = \frac{1}{m_z} \sum_{K \subset \omega_z} \text{curl} \mathbf{u}_h|_K.$$

where \mathbf{L}_h is the tensorial linear Lagrange element space for $d = 3$ (or the linear Lagrange element space for $d = 2$).

Note that the recovery operator C_h preserves P_2 polynomials at the node z :

$$(4.1) \quad (C_h \mathbf{p})(z) = (\text{curl} \mathbf{p})(z), \quad \forall \mathbf{p} \in \mathbf{P}_2(\omega_z).$$

Define $\mathbf{PW}^{3,\infty}(\Omega) := \{\mathbf{v} \in \mathbf{L}^\infty(\Omega) : \mathbf{v}|_K \in \mathbf{W}^{3,\infty}(K), \forall K \in \mathcal{T}_h\}$.

Theorem 4.1. *Let $T\mathbf{f} \in \mathbf{PW}^{3,\infty}(\Omega)$ then there holds the following supercloseness estimation for C_h :*

$$(4.2) \quad \|\text{curl}T\mathbf{f} - C_h T\mathbf{f}\| \lesssim h^2 \|T\mathbf{f}\|_{\mathbf{PW}^{3,\infty}(\Omega)}.$$

Proof. We decompose

$$\text{curl}T\mathbf{f} - C_h T\mathbf{f} = (\text{curl}T\mathbf{f} - (\text{curl}T\mathbf{f})_I) + ((\text{curl}T\mathbf{f})_I - C_h T\mathbf{f})$$

where $(\text{curl}T\mathbf{f})_I \in \mathbf{L}_h$ is the piecewise linear interpolation of $\text{curl}T\mathbf{f}$. By the standard approximation theory,

$$\|\text{curl}T\mathbf{f} - (\text{curl}T\mathbf{f})_I\| \lesssim h^2 \|T\mathbf{f}\|_{\mathbf{PW}^{3,\infty}(\Omega)}.$$

Moreover

$$\begin{aligned} \|(\operatorname{curl}T\mathbf{f})_I - C_h T\mathbf{f}\| &\leq \left(\sum_{K \in \Omega} |K| \sum_{z \in \mathcal{N}_h \cap \bar{K}} \inf_{\mathbf{q}_z \in \mathbf{P}_2(\omega_z)} |C_h(T\mathbf{f} + \mathbf{q}_z)(z) - \operatorname{curl}(T\mathbf{f} + \mathbf{q}_z)(z)|^2 \right)^{1/2} \\ &\lesssim h^2 \|T\mathbf{f}\|_{\mathbf{PW}^{3,\infty}(\Omega)} |\Omega|^{1/2} \lesssim h^2 \|T\mathbf{f}\|_{\mathbf{PW}^{3,\infty}(\Omega)} \end{aligned}$$

where \mathbf{q}_z is an arbitrary quadratic polynomial in ω_z and $C_h \mathbf{q}_z(z) = \operatorname{curl}(\mathbf{q}_z)(z)$. The combination of the above two estimates gives the conclusion. \square

5. NUMERICAL EXPERIMENTS

In this section we provide numerical experiments using the extended linear and quadratic Lagrange elements to support our theoretical work. We generate the FE meshes as the following approach. For the cube and the thick L-shape domain in 3D, we partition the domains into small congruent cubes and then partition each small cube into 12 tetrahedra. For the tetrahedron in 3D, in each mesh refinement we partition each tetrahedron in the mesh into 8 small tetrahedra. We refer the reader to [31] for the detail of the mesh refinement. For the thick L-shape domain and the tetrahedron, the coarse meshes and boundary degrees of freedom in extended quadratic Lagrange element are depicted in Figure 1.

5.1. Numerical results for Maxwell equation. First we shall consider the source problem (3.20) of Maxwell equations in $\Omega = (0, 1)^3$ with the exact solution

$$(5.1) \quad T\mathbf{f} = \begin{pmatrix} \sin(\pi x_1)^3 \sin(\pi x_2)^2 \sin(\pi x_3)^2 \cos(\pi x_2) \cos(\pi x_3) \\ \sin(\pi x_2)^3 \sin(\pi x_3)^2 \sin(\pi x_1)^2 \cos(\pi x_3) \cos(\pi x_1) \\ -2 \sin(\pi x_3)^3 \sin(\pi x_1)^2 \sin(\pi x_2)^2 \cos(\pi x_1) \cos(\pi x_2) \end{pmatrix}.$$

We compute the numerical solution $T_h \mathbf{f}$ and the error $\mathbf{e}_h := T_h \mathbf{f} - T\mathbf{f}$. We also compute the recovery $C_h T_h \mathbf{f}$ of $\operatorname{curl} T_h \mathbf{f}$ and denote the error $\delta C T_h \mathbf{f} := C_h T_h \mathbf{f} - \operatorname{curl} T\mathbf{f}$. The errors of numerical solutions obtained by the extended linear and quadratic Lagrange elements are listed in Table 1. It can be seen that the convergence rates in the $\mathbf{H}(\operatorname{curl})$ -seminorm and the L^2 -norm are about 1 and 2 for the linear and quadratic Lagrange elements, respectively. It is also shown from Table 1 that the recovery $C_h T_h \mathbf{f}$ is a supercloseness to $\operatorname{curl} T_h \mathbf{f}$.

5.2. Numerical results for Maxwell eigenvalues. Let $\{\boldsymbol{\xi}_i\}_{i=1}^{N_1}$ and $\{\boldsymbol{\phi}_i\}_{i=1}^{N_2}$ be the bases of $\mathbf{L}_{h,0}$ and U_h , respectively. The eigenfunction in (2.4) is written as $\mathbf{u}_h = \sum_{i=1}^{N_1} u_i \boldsymbol{\xi}_i + \sum_{i=1}^{N_2} u_{i+N_1} \nabla \boldsymbol{\phi}_i$. Denote $N_h := N_1 + N_2$ and $\vec{u} = (u_1, \dots, u_{N_h})^T$. To describe our algorithm, we specify the following matrices in the discrete case.

Matrix	Dimension	Definition
A_{11}	$N_1 \times N_1$	$A_{11}(l, i) = \int_{\Omega} \operatorname{curl} \boldsymbol{\xi}_i \cdot \operatorname{curl} \boldsymbol{\xi}_l dx$
B_{11}	$N_1 \times N_1$	$B_{11}(l, i) = \int_{\Omega} \boldsymbol{\xi}_i \cdot \boldsymbol{\xi}_l dx$
B_{12}	$N_1 \times N_2$	$B_{12}(l, i) = \int_{\Omega} \nabla \boldsymbol{\phi}_i \cdot \boldsymbol{\xi}_l dx$
B_{22}	$N_2 \times N_2$	$B_{22}(l, i) = \int_{\Omega} \nabla \boldsymbol{\phi}_i \cdot \nabla \boldsymbol{\phi}_l dx$

Then the discretization can be written as the generalized eigenvalue problems

$$A\vec{u} = \lambda B\vec{u}.$$

where

$$(5.2) \quad A := \begin{pmatrix} A_{11} & 0 \\ 0 & 0 \end{pmatrix} \quad \text{and} \quad B := \begin{pmatrix} B_{11} & B_{12} \\ B_{12}^T & B_{22} \end{pmatrix}.$$

In order to give the number of degrees of freedom (Dofs) for the extended Lagrange element methods, we use N , NE , NF , NT to denote the number of nodes, edges, faces and tetrahedra in the mesh. They satisfy the relations $N : NE : NF : NT \approx 1 : 7 : 12 : 6$ in \mathbb{R}^3 and $N : NE : NF \approx 1 : 3 : 2$ in \mathbb{R}^2 . We use NDofs and $\overline{\text{NDofs}}$ to denote the the number of Dofs in the extended Lagrange element methods and the second family of the Nédélec element methods, respectively. For the comparative purpose they are listed in the following table.

	p	$\text{Dim}(\mathbf{L}_{h,0})$	$\text{Dim}(U_h)$	NDofs	$\overline{\text{NDofs}}$
$d = 3$	1	$3N$	$N + NE \approx 8N$	$11N$	$3NE \approx 14N$
	2	$3N + 3NE \approx 24N$	$N + 2NE + NF \approx 27N$	$52N$	$3NE + 3NF \approx 57N$
$d = 2$	1	$2N$	$N + NE \approx 4N$	$6N$	$2NE \approx 6N$
	2	$2N + 2NE \approx 8N$	$N + 2NE + NF \approx 9N$	$17N$	$3NE + 3NT \approx 15N$

The above table shows that the computational complexity of the extended Lagrange element method in 3D is close to but less than the second family of Nédélec element method in 3D when $p = 1, 2$.

Remark 5.1. If $\mathbf{L}_{h,0} \cap \nabla U_h \neq \{\mathbf{0}\}$, there is a nonzero vector \vec{u} such that $\mathbf{u}_h = \mathbf{0}$. Such \vec{u} is exactly an eigenvector of (5.2). We can filter the algebraic spurious eigenvalue λ_h using the following formula

$$\frac{\sqrt{|(\text{curl} \mathbf{u}_h, \text{curl} \mathbf{u}_h) - \lambda_h(\mathbf{u}_h, \mathbf{u}_h)|}}{\|\mathbf{u}_h\|} > \mathcal{E}$$

where \mathcal{E} is the small tolerance.

We now test the new methods for solving the Maxwell eigenvalue problem (2.3). The first eight eigenvalues on different domains are listed as follows:

Unit Square:	π^2	π^2	$2\pi^2$	$4\pi^2$	$4\pi^2$	$5\pi^2$	$5\pi^2$	$8\pi^2$
L-shape:	1.4756218	3.5340314	π^2	π^2	11.389479	12.57219	$2\pi^2$	21.4242598
Unit Cube:	$2\pi^2$	$2\pi^2$	$2\pi^2$	$3\pi^2$	$3\pi^2$	$5\pi^2$	$5\pi^2$	$5\pi^2$
Thick L-shape:	9.63972	11.34523	13.40364	15.19725	19.50933	$2\pi^2$	$2\pi^2$	$2\pi^2$

Let $(\lambda_i, \mathbf{u}_i)$ be the i th Maxwell eigenpair and $(\lambda_{i,h}, \mathbf{u}_{i,h})$ be its approximation obtained by the extended Lagrange FEM. From [20] we have

$$(5.3) \quad \lambda_{i,h} - \lambda_i = \frac{(\text{curl}(\mathbf{u}_{i,h} - \mathbf{u}_i), \text{curl}(\mathbf{u}_{i,h} - \mathbf{u}_i))}{(\mathbf{u}_{i,h}, \mathbf{u}_{i,h})} - \lambda \frac{(\mathbf{u}_{i,h} - \mathbf{u}_i, \mathbf{u}_{i,h} - \mathbf{u}_i)}{(\mathbf{u}_{i,h}, \mathbf{u}_{i,h})}, \quad i = 1, 2, \dots$$

If the eigenfunction \mathbf{u} is smooth, it is expected that $\lambda_{i,h} \geq \lambda_i$ because $\|\mathbf{u}_h - \mathbf{u}\|$ is of higher order than $\|\text{curl}(\mathbf{u}_h - \mathbf{u})\|$.

We first use the extended linear Lagrange FEM to compute for the lowest eight eigenvalues. It can be seen from Tables 2-6 that for the case of the unit square in 2D (c.f. Table 2) and the cube, the tetrahedron and the thick L-shape in 3D (c.f. Tables 4-6), all computed eigenvalues obtained by extended linear Lagrange FEMs present the upper bounds of the associated eigenvalues; so do the numerical eigenvalues $\lambda_{i,h}$ ($i = 2, \dots, 8$) on the L-shape in 2D; however $\lambda_{1,h}$ obtained by the extended linear Lagrange FEM on the L-shape domain does not because the associated eigenfunction \mathbf{u}_1 is strongly unbounded singular. The same is for $\lambda_{2,h}$ obtained by the extended quadratic Lagrange FEM. In all cases given here the convergence rates of the computed eigenvalues by extended linear Lagrange FEM are around 2, which are optimal.

We next use the extended quadratic Lagrange FEM to compute for the lowest eight eigenvalues. It can be seen from Tables 2-6 that for the case of the unit square in 2D (c.f. Table 2) and the cube, the tetrahedron and the thick L-shape in 3D (c.f. Tables 4-6), all computed eigenvalues obtained by extended quadratic Lagrange FEMs present the upper bounds of the associated eigenvalues; so do the numerical eigenvalues $\lambda_{i,h}$ ($i = 3, 4, 5, 7$) on the L-shape in 2D (c.f. Table 3); however $\lambda_{i,h}$ ($i = 1, 2, 6, 8$) obtained by the extended quadratic Lagrange FEM on the L-shape domain does not because of the singularity of the associated eigenfunctions.

The convergence rates of the computed eigenvalues by extended quadratic Lagrange FEM on the square in 2D (c.f. Table 2) and the cube and tetrahedron in 3D (c.f. Tables 4-5) are around 4, which are optimal. However, this is not true for the computed eigenvalue $\lambda_{i,h}$ ($i = 1, 2, 6, 8$) obtained by the extended quadratic Lagrange FEM on the L-shape domain in 2D (c.f. Table 3) and the computed eigenvalue $\lambda_{i,h}$ ($i = 1, 2, 5$) obtained by the extended quadratic Lagrange FEM on the thick L-shape domain in 3D (c.f. Table 6). This is due to the singularity of the associated eigenfunctions.

5.3. Supercloseness lower bound by recovery approach. Using the recovery approach in [32], for the numerical eigenpair $(\lambda_{i,h}, \mathbf{u}_{i,h})$ obtained by the extended linear Lagrange FEM, we shall compute the a-posteriori error estimator of recovery type

$$\eta_h(\mathbf{u}_{i,h}) := \frac{\|\operatorname{curl} \mathbf{u}_{i,h} - C_h \mathbf{u}_{i,h}\|^2}{\|\mathbf{u}_{i,h}\|^2}, \quad i = 1, 2, \dots .$$

Let $\tilde{\lambda}_{i,h} := \lambda_{i,h} - \eta_h(\mathbf{u}_{i,h})$. It is expected that $\tilde{\lambda}_{i,h}$ has the supercloseness property when the eigenfunction \mathbf{u}_i is smooth.

For the case of the unit square in 2D and the cube in 3D, it can be seen from Tables 7 and 9 that $\tilde{\lambda}_{i,h}$ ($i = 1, 2, 3$) are supercloseness lower bounds of λ_i ($i = 1, 2, 3$), respectively.

For the case of the L-shape domain in 2D, we can see from Table 8 that $\tilde{\lambda}_{i,h}$ ($i = 2, 3, 4$) are supercloseness lower bounds of λ_i ($i = 2, 3, 4$), respectively; we can see from Table 3 that $\lambda_{1,h}$ does not present an upper bound of λ_1 because the associated eigenfunction \mathbf{u}_1 is strongly unbounded singular. For this reason the supercloseness property of $\tilde{\lambda}_{1,h}$ is invalid and we do not list $\tilde{\lambda}_{1,h}$.

For the case of the thick L-shape in 3D, we can see from Table 9 that $\tilde{\lambda}_{i,h}$ ($i = 1, 2, 3$) are lower bounds of λ_i ($i = 1, 2, 3$), respectively, and meanwhile $\tilde{\lambda}_{3,h}$ is a supercloseness of λ_3 . $\tilde{\lambda}_{1,h}$ and $\tilde{\lambda}_{2,h}$ do not supercloseness property due to the singularity of the eigenfunctions \mathbf{u}_1 and \mathbf{u}_2 .

TABLE 1. Error for the solution in (3.20) on the unit cube using extended linear (left) and quadratic (right) Lagrange finite element methods.

h	1/2	1/4	1/6	1/8	1/10	1/2	1/3	1/4	1/5	1/6
$\ \operatorname{curl}(\mathbf{e}_h)\ $	0.7516	0.4818	0.3351	0.2556	0.2062	0.425	0.2291	0.1168	0.0769	0.0544
Rate	–	0.64	0.90	0.94	0.96	–	1.52	2.34	1.87	1.90
$\ \mathbf{e}_h\ $	0.0555	0.0244	0.0117	0.0067	0.0044	0.017	0.0059	0.0023	0.0012	7.38E-04
Rate	–	1.19	1.81	1.94	1.88	–	2.61	3.27	2.92	2.67
$\ \delta C \operatorname{curl} T_h \mathbf{f}\ $	0.8063	0.3778	0.1363	0.056	0.0266					
Rate	–	1.09	2.51	3.09	3.34					

TABLE 2. Numerical eigenvalues on the unit square obtained by extended linear (left) and quadratic (right) Lagrange finite element methods.

h	1/4	1/8	1/16	1/32	1/4	1/8	1/16	1/32
$\lambda_{1,h}$	10.0918	9.92542	9.88357	9.87310	9.8712349	9.8697136	9.8696108	9.8696048
Rate	–	1.99↓	2.00↓	2.00↓	–	3.90↓	4.08↓	4.00↓
$\lambda_{2,h}$	10.1067↓	9.92907↓	9.88448↓	9.87332↓	9.8713258	9.8697073	9.8696112	9.8696048
Rate	–	2.00↓	2.00↓	2.00↓	–	4.06↓	3.91↓	4.00↓
$\lambda_{3,h}$	20.7531	19.9912	19.8021	19.7549	19.750518	19.73995	19.739256	19.739211
Rate	–	2.01↓	2.00↓	2.00↓	–	3.92↓	3.98↓	4.00↓
$\lambda_{4,h}$	43.1269	40.4107	39.7121	39.5368	39.574996	39.484880	39.478789	39.478443
Rate	–	1.97↓	2.00↓	2.00↓	–	3.90↓	4.12↓	3.85↓
$\lambda_{5,h}$	43.3726	40.4638	39.7252	39.5401	39.566074	39.484259	39.478828	39.478440
Rate	–	1.98↓	2.00↓	2.00↓	–	3.91↓	3.83↓	4.14↓
$\lambda_{6,h}$	55.4626	50.8812	49.7304	49.4435	49.514075	49.359361	49.348848	49.348067
Rate	–	2.00↓	2.00↓	2.00↓	–	3.87↓	3.78↓	4.18↓
$\lambda_{7,h}$	55.9247	50.9809	49.7541	49.4494	49.534035	49.360921	49.348748	49.348074
Rate	–	2.01↓	2.01↓	2.00↓	–	3.85↓	4.15↓	3.80↓
$\lambda_{8,h}$	94.8772	83.0772	79.9849	79.2136	79.639538	79.005160	78.959969	78.957032
Rate	–	1.95↓	2.00↓	2.00↓	–	3.82↓	3.95↓	3.99↓

TABLE 3. Numerical eigenvalues on the L-shape domain obtained by extended linear (left) and quadratic (right) Lagrange finite element methods.

h	1/4	1/8	1/16	1/32	1/64	1/4	1/8	1/16	1/32
$\lambda_{1,h}$	1.4777	1.47511	1.47508	1.47532	1.47548	1.47278	1.474489	1.475171	1.475443
Rate	–	2.49↓	-0.12↓	1.17↑	2.52↑	–	1.41↑	1.58↑	2.27↑
$\lambda_{2,h}$	3.5694	3.54292	3.53630	3.53459	3.53417	3.53407	3.534029	3.5340305	3.5340312
Rate	–	2.00↓	1.97↓	2.02↓	2.00↓	–	4.63↓	1.08↑	2.32↑
$\lambda_{3,h}$	10.095	9.92637	9.88380	9.87316	9.87049	9.87118	9.869704	9.8696106	9.8696048
Rate	–	1.99↓	2.00↓	2.00↓	2.00↓	–	3.99↓	4.00↓	4.00↓
$\lambda_{4,h}$	10.132	9.93564	9.88610	9.87374	9.87064	9.87201	9.869756	9.8696139	9.8696050
Rate	–	1.99↓	2.00↓	2.00↓	2.00↓	–	3.98↓	3.99↓	4.00↓
$\lambda_{5,h}$	11.699	11.4677	11.4091	11.3943	11.3907	11.3926	11.38967	11.38949	11.38947
Rate	–	1.98↓	2.00↓	2.00↓	2.00↓	–	4.03↓	4.12↓	4.36↓
$\lambda_{6,h}$	12.933	12.6608	12.5933	12.5770	12.5733	12.5674	12.56899	12.57094	12.57181
Rate	–	2.03↓	2.07↓	2.11↓	2.08↓	–	0.58↑	1.36↑	1.71↑
$\lambda_{7,h}$	20.758	19.9959	19.8035	19.7552	19.7432	19.7525	19.74008	19.73926	19.73921
Rate	–	1.99↓	2.00↓	2.00↓	2.00↓	–	3.92↓	3.98↓	4.00↓
$\lambda_{8,h}$	22.598	21.7148	21.4944	21.4409	21.4282	21.4232	21.41747	21.42140	21.42338
Rate	–	2.01↓	2.05↓	2.07↓	2.05↓	–	-2.74↓	1.25↑	1.70↑

6. CONCLUSION

In this paper, we proposed a new method using Lagrange element space to solve the Maxwell equations and the associated eigenvalue problem. To obtain numerical solution of supercloseness, we propose an average type curl recovery scheme for the extended linear lagrange FEM. This scheme can be used to obtain the numerical lower bound of Maxwell eigenvalues. Although we only focus on the Maxwell equation and its eigenvalue problem with constant coefficients, the new method and the associated theoretical results are suitable for discontinuous coefficients.

TABLE 4. Numerical eigenvalues on the unit cube obtained by extended linear (left) and quadratic (right) Lagrange finite element methods.

h	1/2	1/3	1/4	1/5	1/6	1/2	1/3	1/4	1/5	1/6
$\lambda_{1,h}$	24.6853	21.6648	20.7846	20.3917	20.1865	19.879	19.7648	19.7468	19.7421	19.7406
Rate	–	2.33↓	2.12↓	2.11↓	2.07↓	–	4.19↓	4.22↓	4.33↓	4.01↓
$\lambda_{2,h}$	24.7298	21.7094	20.7907	20.3935	20.1886	19.8836	19.7659	19.7468	19.7422	19.7406
Rate	–	2.29↓	2.18↓	2.13↓	2.06↓	–	4.16↓	4.37↓	4.17↓	4.2↓
$\lambda_{3,h}$	24.7577	21.7018	20.7935	20.396	20.1902	19.886	19.7659	19.7469	19.7422	19.7406
Rate	–	2.32↓	2.16↓	2.12↓	2.06↓	–	4.20↓	4.33↓	4.23↓	4.20↓
$\lambda_{4,h}$	39.9657	33.1761	31.4867	30.7537	30.3871	30.0109	29.6946	29.6345	29.6189	29.6134
Rate	–	2.63↓	2.23↓	2.22↓	2.12↓	–	3.81↓	4.19↓	4.19↓	4.32↓
$\lambda_{5,h}$	39.9684	33.301	31.5064	30.7633	30.396	30.0139	29.6966	29.6347	29.619	29.6134
Rate	–	2.54↓	2.31↓	2.23↓	2.1↓	–	3.77↓	4.24↓	4.18↓	4.38↓
$\lambda_{6,h}$	74.4975	61.1531	56.009	53.5104	52.2029	50.9636	49.6862	49.4548	49.3926	49.3697
Rate	–	1.87↓	1.99↓	2.11↓	2.07↓	–	3.86↓	4.01↓	3.91↓	3.95↓
$\lambda_{7,h}$	74.6583	61.356	56.0925	53.539	52.2052	51.0757	49.6884	49.4561	49.3931	49.3699
Rate	–	1.84↓	2.01↓	2.13↓	2.10↓	–	4.01↓	3.99↓	3.92↓	3.97↓
$\lambda_{8,h}$	74.7468	61.7022	56.1204	53.5613	52.2208	51.1667	49.6958	49.4577	49.3935	49.3699
Rate	–	1.78↓	2.09↓	2.13↓	2.10↓	–	4.08↓	4.01↓	3.95↓	4.01↓

TABLE 5. Numerical eigenvalues on the tetrahedron obtained by extended linear (left) and quadratic (right) Lagrange finite element methods.

h	1/2	1/4	1/8	1/16	1/4	1/8	1/16	1/32
$\lambda_{1,h}$	32.3467	27.6752	26.46	26.156	26.532	26.2471	26.0698	26.0557
Rate	–	1.96↓	2.00↓	2.01↓	–	1.32↓	3.76↓	3.65↓
$\lambda_{2,h}$	33.079	27.7695	26.4806	26.161	27.7558	26.2883	26.0726	26.0559
Rate	–	2.04↓	2.01↓	2.01↓	–	2.87↓	3.8↓	3.69↓
$\lambda_{3,h}$	33.079	27.7695	26.4806	26.161	27.7558	26.2883	26.0726	26.0559
Rate	–	2.04↓	2.01↓	2.01↓	–	2.87↓	3.8↓	3.69↓
$\lambda_{4,h}$	80.8141	60.8229	55.2449	53.8868	70.0000	54.9355	53.5601	53.446
Rate	–	1.89↓	2.04↓	2.03↓	–	3.47↓	3.71↓	3.59↓
$\lambda_{5,h}$	81.3878	61.3432	55.4132	53.9318	70.8989	54.9545	53.5859	53.448
Rate	–	1.82↓	2.01↓	2.02↓	–	3.53↓	3.45↓	3.31↓
$\lambda_{6,h}$	81.3878	61.3432	55.4132	53.9318	74.6667	54.9545	53.5859	53.448
Rate	–	1.82↓	2.01↓	2.02↓	–	3.82↓	3.45↓	3.31↓
$\lambda_{7,h}$	81.5981	63.3483	58.5518	57.3607	76.6727	58.6841	57.1064	56.9740
Rate	–	1.95↓	2.01↓	2.03↓	–	3.53↓	3.69↓	3.58↓
$\lambda_{8,h}$	85.5942	64.6753	58.9099	57.4519	76.6727	58.8057	57.1416	56.9769
Rate	–	1.89↓	1.99↓	2.02↓	–	3.43↓	3.47↓	3.34↓

REFERENCES

- [1] J. C. NÉDÉLEC, *Mixed finite elements in R^3* , Numer. Math., 35(1980), 315–341.
- [2] D. BOFFI, *Finite Element approximation of eigenvalue problems*, Acta Numerica, 19(2010), 1–120.
- [3] D. N. ARNOLD, R. S. FALK, AND R. WINTHER, *Finite element exterior calculus, homological techniques, and applications*, Acta Numerica, (2006), 1–155.
- [4] A. BONITO AND J. -L. GUERMOND, *Approximation of the eigenvalue problem for the time harmonic Maxwell system by continuous Lagrange finite elements*, Math. Comp., 80 (2011), 1887–1910.
- [5] S. BADIA AND R. CODINA, *A nodal-based finite element approximation of the Maxwell problem suitable for singular solutions*, SIAM J. Numer. Anal., 50 (2012), 398–417.
- [6] A. BUFFA, P. CIARLET, AND E. JAMELOT, *Solving electromagnetic eigenvalue problems in polyhedral domains with nodal finite elements*, Nume. Math., 113 (2009), 497–518.

TABLE 6. Numerical eigenvalues on the thick L-shape domain obtained by extended linear (left) and quadratic (right) Lagrange finite element methods.

h	1/2	1/3	1/4	1/5	1/6	1/2	1/3	1/4	1/5	1/6
$\lambda_{1,h}$	11.091	10.341	10.0498	9.9144	9.8393	9.7357	9.6882	9.6717	9.6632	9.658
<i>Rate</i>	–	1.79↓	1.87↓	1.80↓	1.75↓	–	1.68↓	1.45↓	1.38↓	1.37↓
$\lambda_{2,h}$	14.0532	12.5497	12.0375	11.7989	11.6686	11.4258	11.3765	11.3635	11.3579	11.3548
<i>Rate</i>	–	2.00↓	1.93↓	1.89↓	1.86↓	–	2.33↓	1.87↓	1.64↓	1.54↓
$\lambda_{3,h}$	15.3133	14.2097	13.8451	13.6809	13.5949	13.4498	13.4121	13.4063	13.4048	13.4042
<i>Rate</i>	–	2.13↓	2.09↓	2.08↓	2.04↓	–	4.18↓	4.02↓	3.71↓	3.97↓
$\lambda_{4,h}$	17.6559	16.2547	15.7792	15.5624	15.4465	15.2731	15.2126	15.2025	15.1996	15.1985
<i>Rate</i>	–	2.08↓	2.08↓	2.09↓	2.09↓	–	3.94↓	3.73↓	3.6↓	3.47↓
$\lambda_{5,h}$	23.9564	21.6577	20.7545	20.3179	20.0812	19.7751	19.6082	19.5667	19.5492	19.5393
<i>Rate</i>	–	1.79↓	1.9↓	1.93↓	1.9↓	–	2.44↓	1.89↓	1.63↓	1.57↓
$\lambda_{6,h}$	24.046	21.6728	20.7908	20.3998	20.1912	19.8665	19.7619	19.7461	19.7419	19.7405
<i>Rate</i>	–	1.98↓	2.12↓	2.08↓	2.08↓	–	4.25↓	4.14↓	4.21↓	4.03↓
$\lambda_{7,h}$	24.4227	21.7218	20.7969	20.4008	20.1916	19.869	19.7626	19.7461	19.7419	19.7405
<i>Rate</i>	–	2.12↓	2.18↓	2.10↓	2.08↓	–	4.23↓	4.25↓	4.21↓	4.03↓
$\lambda_{8,h}$	24.7486	21.7637	20.8081	20.4013	20.1924	19.8817	19.7631	19.7463	19.7421	19.7405
<i>Rate</i>	–	2.23↓	2.22↓	2.15↓	2.08↓	–	4.40↓	4.22↓	4.02↓	4.42↓

TABLE 7. Recovered discrete eigenvalues on the square.

h	1/4	1/8	1/16	1/32	1/64
$\tilde{\lambda}_{1,h}$	9.79974	9.86602	9.86933	9.86958	9.86960
<i>Rate</i>	–	4.28↑	3.71↑	3.56↑	3.42↑
$\tilde{\lambda}_{2,h}$	19.24442	19.70742	19.73691	19.73903	19.73919
<i>Rate</i>	–	3.96↑	3.79↑	3.69↑	3.56↑
$\tilde{\lambda}_{3,h}$	35.99717	39.21930	39.46352	39.47736	39.47834
<i>Rate</i>	–	3.75↑	4.12↑	3.82↑	3.79↑

TABLE 8. Recovered discrete eigenvalues on the L-shape domain.

h	1/4	1/8	1/16	1/32	1/64
$\tilde{\lambda}_{2,h}$	3.532018	3.533785	3.534006	3.534028	3.534031
<i>Rate</i>	–	3.03↑	3.25↑	3.10↑	2.96↑
$\tilde{\lambda}_{3,h}$	9.82203	9.86564	9.86929	9.86958	9.86960
<i>Rate</i>	–	3.59↑	3.64↑	3.54↑	3.40↑
$\tilde{\lambda}_{4,h}$	11.29961	11.38192	11.38890	11.38943	11.38948
<i>Rate</i>	–	3.57↑	3.70↑	3.64↑	3.51↑

TABLE 9. Recovered discrete eigenvalues on the cube (left) and the thick L-shape domain (right).

h	1/4	1/8	1/16	1/32	1/64	1/3	1/4	1/5	1/6
$\lambda_{1,h}$	9.79974	9.86602	9.86933	9.86958	9.86960	9.345	9.5008	9.5555	9.5826
<i>Rate</i>	–	4.28↑	3.71↑	3.56↑	3.42↑	–	2.61↑	2.24↑	2.13↑
$\tilde{\lambda}_{2,h}$	19.24442	19.70742	19.73691	19.73903	19.73919	11.0998	11.2155	11.2574	11.2809
<i>Rate</i>	–	3.96↑	3.79↑	3.69↑	3.56↑	–	2.22↑	1.75↑	1.71↑
$\tilde{\lambda}_{3,h}$	35.99716	39.21929	39.46352	39.47736	39.47834	13.1075	13.2933	13.3529	13.3767
<i>Rate</i>	–	3.75↑	4.12↑	3.82↑	3.79↑	–	3.43↑	3.48↑	3.47↑

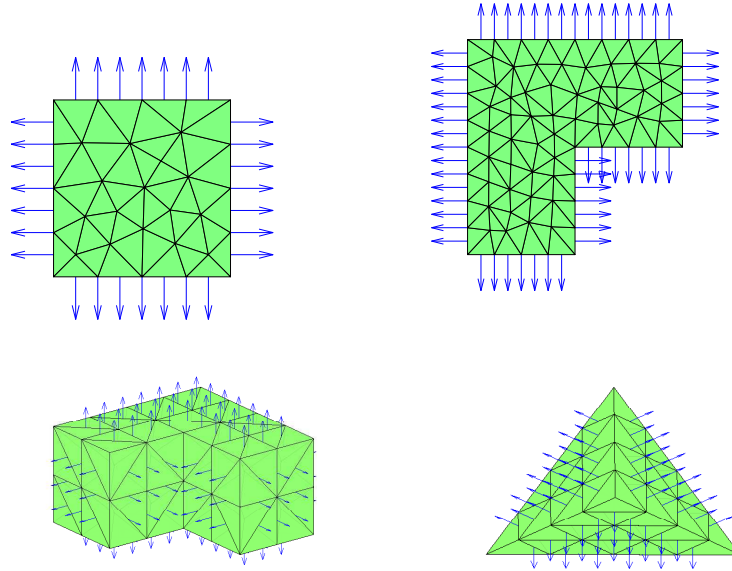


FIGURE 1. Coarse meshes and degrees of freedom on $\partial\Omega$ for extended quadratic Lagrange elements in 2D and 3D.

- [7] H. DUAN, W. LIU, J. MA, R. C. TAN, AND S. ZHANG, *A family of optimal Lagrange elements for Maxwell equations*, J. Comp. Appl. Math., 358 (2019), 241–265.
- [8] S. H. WONG AND Z. CENDES, *Combined finite element-modal solution of three-dimensional eddy current problems*, IEEE Transactions on Magnetics, 24 (1988), 2685–2687.
- [9] M. J. POWELL AND M. A. SABIN, *Piecewise quadratic approximations on triangles*, ACM Transactions on Mathematical Software (TOMS), 3 (1977), 316–325.
- [10] A. WORSEY AND G. FARIN, *An n -dimensional Clough-Tocher interpolant*, Constructive Approximation, 3 (1987), 99–110.
- [11] D. BOFFI, J. GUZMÁN, AND M. NEILAN, *Convergence of Lagrange finite elements for the Maxwell eigenvalue problem in two dimensions*, IMA J. Numer. Anal., (2022), 10.1093/imanum/drab104.
- [12] D. BOFFI, J. GUZMÁN, AND M. NEILAN, *Convergence of Lagrange finite element methods for Maxwell eigenvalue problem in 3D*, (2022), arXiv:2204.10876 [math.NA].
- [13] K. HU, Q. ZHANG, J. HAN, L. WANG, AND Z. ZHANG, *Spurious solutions for high order curl problems*, IMA Journal of Numerical Analysis, 111(2022), 1-28.
- [14] J. HU, K. HU, AND Q. ZHANG, *Partially discontinuous nodal finite elements for $H(\text{curl})$ and $H(\text{div})$* , Comput. Methods Appl. Math., 22 (2022), 613-629.
- [15] P. MONK, *Finite Element Methods for Maxwell's Equations*, Oxford University Press, Oxford, UK, 2003.
- [16] D. BOFFI, P. FERNANDES, L. GASTALDI, AND I. PERUGIA, *Computational Models of Electromagnetic Resonators: Analysis of Edge Element Approximation*, SIAM Journal on Numerical Analysis, 36 (1999), 1264–1290.
- [17] R. HIPTMAIR, *Finite elements in computational electromagnetism*, Acta Numer., 11 (2002), 237-339.
- [18] W. XIAO AND J. SUN, *Band structure calculation of photonic crystals with frequency-dependent permittivities*, J. Optical Society of America A, 38 (2021), 628-633.
- [19] B. GONG, J. SUN, AND X. WU, *Finite element approximation of the modified Maxwell's Stekloff eigenvalues*, SIAM J. Numer. Anal., 59 (2021).
- [20] I. BABUSKA AND J. OSBORN, *Eigenvalue Problems*, in: P. G. Ciarlet, J. L. Lions, (Ed.), *Finite Element Methods (Part 1)*, Handbook of Numerical Analysis, vol.2, north-holand: Elsevier science publishers, 1991, 640-787.

- [21] D. GALLISTL AND V. OLKHOVSKIY, *Computational lower bounds of the Maxwell eigenvalues*, SIAM J. Numer. Anal., 61(2023), 539-561.
- [22] Y. YANG, Z. ZHANG, F. LIN, *Eigenvalue approximation from below using non-conforming finite elements*, Sci. China Math., 137-150, 53(2010).
- [23] J. HU, Y. HUANG AND Q. LIN, *Lower bounds for eigenvalues of elliptic operators: by nonconforming finite element methods*, J. Sci. Comput., 61(2014), 196-221.
- [24] C. CARSTENSEN AND D. GALLISTL, *Guaranteed lower eigenvalue bounds for the biharmonic equation*. Numer. Math. 126, 33–51 (2014).
- [25] C. YOU, H. XIE AND X. LIU, *Guaranteed eigenvalue bounds for the Steklov eigenvalue problem*, SIAM J. Numer. Anal., 57(3) (2019), 1395-1410.
- [26] P. CLÉMENT, *Approximation by finite element functions using local regularization*, RAIRO Anal. Numer., R-2(1975), 77-84.
- [27] C. AMROUCHE, C. BERNARDI, M. DAUGE AND V. GIRAULT, *Vector potentials in three-dimensional non-smooth domains*, Math. Meth. Appl. Sci., 21(1998), 823-864.
- [28] M. COSTABEL, M. DAUGE, *Weighted regularization of Maxwell equations in polyhedral domains*, Numer. Math., 93(2002), 239-277.
- [29] F. CHATELIN, *Spectral Approximations of Linear Operators*, Academic Press, New York, 1983.
- [30] Y. HUANG, J. LI, C. WU, W. YANG, *Superconvergence analysis for linear tetrahedral edge elements*, J. Sci. Comput. 62(2015), 122-145.
- [31] L. CHEN, *iFEM: An Integrated Finite Element Methods Package in MATLAB*, Technical report, University of California at Irvine, 2009.
- [32] A. NAGA, Z. ZHANG AND A. ZHOU, *Enhancing eigenvalue approximation by gradient recovery*, SIAM J. Sci. Comput., 28 (2006), 1289-1300.

SCHOOL OF MATHEMATICAL SCIENCES, GUIZHOU NORMAL UNIVERSITY, GUIYANG, 550025
Email address: hanjiayu@gznu.edu.cn, hanjiayu126@126.com